Separation Science and Technology
Publication details, including instructions for authors and subscription information:
http://www.informaworld.com/smpp/title~content=t713708471

Analysis of Parameters for Ion Permeation in Immobilized Liquid Membranes. I. Perfect-Mix Stages and Cascades

F. P. McCandless[a]
[a] DEPARTMENT OF CHEMICAL ENGINEERING, MONTANA STATE UNIVERSITY, BOZEMAN, MONTANA, USA

To cite this Article McCandless, F. P.(1997) 'Analysis of Parameters for Ion Permeation in Immobilized Liquid Membranes. I. Perfect-Mix Stages and Cascades', Separation Science and Technology, 32: 17, 2785 — 2806

To link to this Article: DOI: 10.1080/01496399708002222

URL: http://dx.doi.org/10.1080/01496399708002222

SEPARATION SCIENCE AND TECHNOLOGY, **32**(17), pp. 2785–2806, 1997

Analysis of Parameters for Ion Permeation in Immobilized Liquid Membranes. I. Perfect-Mix Stages and Cascades

F. P. McCANDLESS
DEPARTMENT OF CHEMICAL ENGINEERING
MONTANA STATE UNIVERSITY
BOZEMAN, MONTANA 59717, USA

ABSTRACT

This study is concerned with the engineering design and analysis of systems for which the basis for separation is the selective permeation of dissociated salts from aqueous feed to strip solutions through immobilized liquid membranes. Theoretical equations are derived for binary mixtures, assuming Fick's law, to model perfect-mix permeation stages, and separation cascades containing perfect-mix stages. The results should apply both to passive (ordinary) diffusion and macrocycle-mediated transport. Important stage variables include the ratio of total dissociated salt concentrations in the stage feed and strip solutions, the total concentration in the stage strip solution, the stage cut, and the ratio of permeability coefficients for the two species in the separation mixture, i.e., the ideal separation factor. The stage separation factor is a complex function of these variables, and may be much less than the ideal separation factor, depending on values of these variables. Severe stagewise diffusional limitations can exist, particularly if the feed solution must be stripped to very low concentration levels. A conceptual design for an ion permeation cascade is presented which suggests that the overall ion permeation process is quite complex and may be energy intensive. For many separations, cascading is required to achieve desired separations, even with very large ideal separation factors.

INTRODUCTION AND BACKGROUND

The use of immobilized liquid membranes (ILMs) to transport metal ions selectively from a mixture was first proposed over 30 years ago (1). Since then many studies have been carried out on the transport and separation properties of these immobilized liquid membranes. Suggested possible uses range from the recovery of metals such as Ag, Cu, Cr, Co, Ni, Pb, etc. from various industrial solutions, to decontamination of high level radioactive wastes, and environmental remediation. However, to our knowledge, no one has previously carried out engineering design and analysis for the separation of binary mixtures of dissociated salts (ions) by permeation through ILMs, hence this paper. The application of these design and analysis principles will determine process peculiarities, permit the calculation of stage and cascade requirements to obtain desired separations, and help better define systems in which ion diffusion could be a useful separation unit operation.

In this paper we will be concerned with two types of ion permeation: ordinary (passive) diffusion and the selective transport of ions through ILMs using materials such as crown ethers as carriers, i.e., "facilitated" or "macrocycle-mediated" transport. The present study does not address the case of coupled transport membranes in which metal ions can be "chemically pumped" from dilute to concentrated solutions.

For this "first look" at ion permeation analysis it is convenient to assume the separation is of a binary mixture and that the stages are perfect-mix. Later, the concepts may be extended to separations between "key" components in more complex mixtures, to multi-component mixtures, and to other stage flow configurations. In any case, the binary perfect-mix study should give a good indication of the technical feasibility of the application of ion permeation to specific separation problems.

Consider the perfect-mix ion permeation separation stage shown schematically in Fig. 1.

In this perfect-mix stage it is assumed that the rate of mixing on the feed side of the membrane is so rapid, as compared with the flow rate, that the tails stream leaving the stage has the same total concentration $[C^t_T)_i]$ and composition (x_i) as the fluid on the feed side of the membrane, i.e., $(C^t_F)_i$ and x_i, which are assumed to be constant at all points on the feed side of the membrane. The same assumption is made for the strip side and heads stream where $(C^t_H)_l = (C^t_S)_i$. In this stage terminology the *heads* stream is the one enriched in the desired species, while the *tails* stream is the one depleted in the desired species.

In this stage a solution containing the feed ions, rate Z_i, concentration $(C^t_P)_{i,\text{in}}$, mole fraction z_i is fed to one side of the membrane, while a strip solution, rate S_i, of deionized water $[(C^t_S)_{i,\text{in}} = 0]$ is fed to the other side. During the stage process some of the dissociated salts (or ion pairs) permeate from the feed to the strip solution and, as a result, the ion fraction of the more permeable species is increased in the strip phase relative to that in the feed phase from x_i to y_i, while the ion fraction of the less

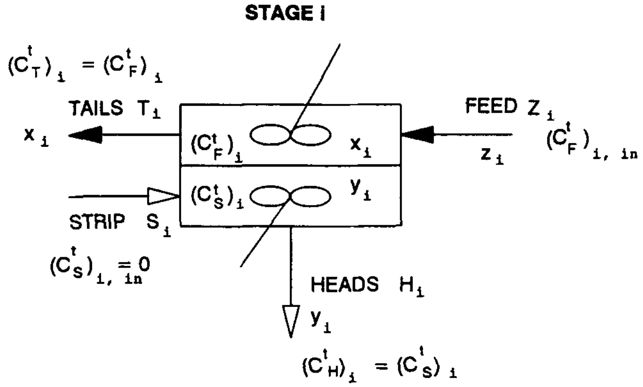

FIG. 1 Schematic diagram of a perfect-mix ion permeation stage.

permeable species is increased in the feed phase, and that of the more permeable ions is decreased from z_i to x_i. During this process the total ion concentration in the strip phase *increases* from 0 to $(C^t_S)_i$, with a concomitant *decrease* in the feed total ion concentration. In discussions that follow, all molar rates (Z_i, H_i, T_i) and mole fractions are on a solvent-free basis.

As indicated by the above discussion, in many respects separation by ion permeation is quite similar to the more familiar gas permeation and gas diffusion processes, in that diffusion across the membrane occurs because of a difference in free energy or thermodynamic activity (concentration) on the two sides of the membrane. In the gaseous processes this driving force for diffusion is established and maintained by adjusting the pressure on the two sides of the membrane so that the permeate side is at a suitably lower pressure than the feed side. In these gaseous processes some of all of the species present in the feed mixture permeate through the membrane, but at different rates, which is the basis for separation. However, in ion permeation only the dissociated salts permeate through the membrane phase; the solvent, which fixes concentration, does not. In most cases in ion permeation, some of all of the species present in the feed solution will permeate through the membrane phase but at different rates, which, like gas diffusion, is the basis for separation. In this case the concentration difference necessary for the diffusion process to take place must be established by adjusting the amount of solvent relative to solute present in the feed and permeate (strip) solutions.

Many of the developments that follow are similar to, and rely on, the teachings of Stern and Walawender (2) and Naylor and Backer (5) who applied separation science principles to gas permeation, and to Benedict (3, 4) who developed much of modern separation cascade theory.

STAGE SEPARATION FACTORS IN ION PERMEATION

The (limited) degree of separation that is obtained in a single stage depends on the relative permeabilities of the different ion species, membrane area, the fraction of the feed that is allowed to permeate (i.e., the "cut"), feed and strip solution concentrations and rates, and the flow pattern of feed and strip phases within the stage. These variables are related in a complex manner.

In developments that follow it is assumed that: 1) the liquids on the two sides of the membrane are ideal solutions; activities can be represented by concentrations and mole fractions, 2) the same solvent is used on the two sides of the membrane, and 3) the pressures on the two sides of the membrane are the same.

The transport model that has been successfully used to analyze the results of transport experiments for both passive diffusion and macrocycle-mediated cation transport is based on Fick's law (6, 7). Thus, it is assumed that the rates of permeation obey Fick's law which takes on the following forms under steady-state conditions for the perfect-mix stage:

$$(J_i^{\mathrm{A}})(a_i) - (C_{\mathrm{S}}^{\mathrm{A}})_i(S_i) = (P^{\mathrm{A}})(a_i)[(C_{\mathrm{F}}^{\mathrm{A}})_i - (C_{\mathrm{S}}^{\mathrm{A}})_i] \tag{1}$$

$$(J_i^{\mathrm{B}})(a_i) - (C_{\mathrm{S}}^{\mathrm{B}})_i(S_i) = (P^{\mathrm{B}})(a_i)[(C_{\mathrm{F}}^{\mathrm{B}})_i - (C_{\mathrm{S}}^{\mathrm{B}})_i] \tag{2}$$

Here, the superscripts A and B refer to species A and B in the binary mixture, J and P are the flux and permeability coefficients, respectively, for the specific dissociated salts, a_i is the area of stage i, and S_i is the volumetric strip solution rate in stage i. The concentration of the two species are related to the total ion concentration by

$$\begin{aligned} (C_{\mathrm{S}}^{\mathrm{A}})_i &= (C_{\mathrm{S}}^{\mathrm{t}})_i y_i \\ (C_{\mathrm{S}}^{\mathrm{B}})_i &= (C_{\mathrm{S}}^{\mathrm{t}})_i(1 - y_i) \\ (C_{\mathrm{F}}^{\mathrm{A}})_i &= (C_{\mathrm{F}}^{\mathrm{t}})_i x_i \\ (C_{\mathrm{F}}^{\mathrm{B}})_i &= (C_{\mathrm{F}}^{\mathrm{t}})_i(1 - x_i) \end{aligned} \tag{3}$$

Dividing Eq. (1) by Eq. (2) gives

$$\frac{(C_{\mathrm{S}}^{\mathrm{A}})_i}{(C_{\mathrm{S}}^{\mathrm{B}})_i} = \frac{P^{\mathrm{A}}}{P^{\mathrm{B}}}\left[\frac{(C_{\mathrm{F}}^{\mathrm{A}})_i - (C_{\mathrm{S}}^{\mathrm{A}})_i}{(C_{\mathrm{F}}^{\mathrm{B}})_i - (C_{\mathrm{S}}^{\mathrm{B}})_i}\right] \tag{4}$$

The ratio of the permeability coefficients

$$P^{A}/P^{B} \equiv \alpha^* \tag{5}$$

is the *ideal* separation factor and depends only on the characteristics of the two permeating species in the particular membrane phase.

The stage separation factor for a binary mixture is defined in the usual way:

$$\alpha_i = \frac{y_i(1 - x_i)}{x_i(1 - y_i)} \tag{6a}$$

$$y_i = \frac{\alpha_i x_i}{1 + (\alpha_i - 1)x_i} \tag{6b}$$

Substitution of Eqs. (3), (5), and (6a) into Eq. (4) gives

$$\frac{y_i}{1 - y_i} = \alpha^* \left[\frac{x_i - \dfrac{1}{r} y_i}{1 - x_i - \dfrac{1}{r}(1 - y_i)} \right] \tag{7}$$

where r is the ratio of the *total* ion concentration on the two sides of the membrane:

$$r = (C_F^t)_i/(C_S^t)_i \tag{8}$$

Alternatively, Eq. (6b) can be used to obtain

$$\alpha_i = \alpha^* \left[\frac{\left(\dfrac{1 - x_i}{1 - y_i}\right)}{\left(\dfrac{1 - x_i}{1 - y_i}\right) + \dfrac{1}{r}(\alpha^* - 1)} \right] \tag{9}$$

Also, from Eq. (7) it follows that

$$y_i = \frac{(\alpha^* - 1)(rx_i + 1) + r - \sqrt{[(\alpha^* - 1)(rx_i + 1) + r]^2 - 4(\alpha^* - 1)(\alpha^*)(r)(x_i)}}{2(\alpha^* - 1)} \tag{10}$$

or

$$x_i = \frac{ry_i + (\alpha^* - 1)(1 - y_i)(y_i)}{r[\alpha^*(1 - y_i) + y_i]} \tag{11}$$

From Eq. (9) it can be seen that the stage separation factor, α_i, depends on the ideal separation factor, α^*, the total ion concentration ratio, r, and

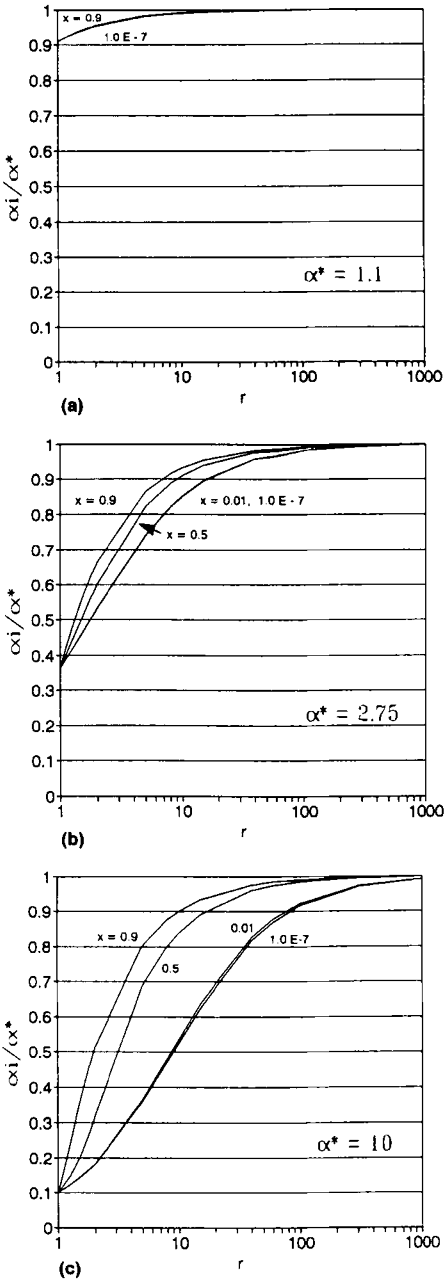

FIG. 2 α_i/α^* as a function of r for different α^*, and stage feed side compositions.

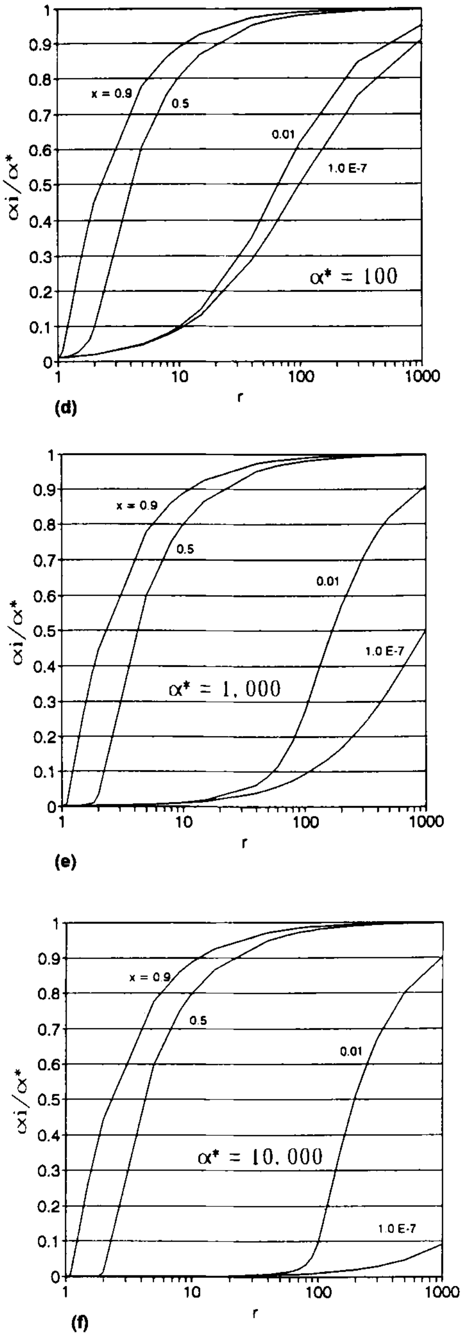

FIG. 2 Continued.

on the stage compositions in terms of mole fractions of ions on the two sides of the stage membrane.

It is interesting to see how α_i varies with r for different values of x_i, and for various α^*. This is easily done by solving Eq. (7) for y_i for specified values of α^*, x_i, and r; and then for α_i using either Eq. (6a) or (9). Figures (2a) through (2f) present the results for r in the range 1 to 1000, for x = 0.9, 0.5, and 0.01, and 1×10^{-7} for $\alpha^* = 1.1$, 2.75, 10, 100, 1000, and 10,000. Although the choice of α^* to investigate is rather arbitrary, α^* for ordinary diffusion is usually in the range $1 < \alpha^* < 5$, while α^* may be in the range of 100 to as high as ~10,000 for macrocycle-mediated transport (7, 8). Intermediate values are included to show trends.

As is evident from Eq. (9), as $r \rightarrow 1$, $\alpha_i \rightarrow 1$, $y_i \rightarrow x_i$, and $\alpha_i/\alpha^* \rightarrow 1/\alpha^*$ for all $\alpha^* > 1$ and, in general as r is made large, $\alpha_i \rightarrow \alpha^*$. However, significantly, for small x_i the ratio α_i/α^* can be much less than 1 even for large r for higher values of α^*. For very small x_i (and hence y_i), $\alpha_i/\alpha^* \rightarrow r/(r + \alpha^* - 1)$, which can be small depending on r and α^*. This is clearly shown in Figs. (2e) and (2f). Since C^t_F is limited by solubility, very large values of r can only be obtained by using very dilute strip solutions.

In developments that follow, A is the more permeable species and B the less permeable species. Two hypothetical binary separations are considered:

1. The separation of a feed containing 50 mol % of each species (x_F = 0.5) to produce $y_P \geq 0.99$ and $x_W \leq 0.01$.
2. The "decontamination" of a dilute binary mixture in which it is assumed that $x_F = 1 \times 10^{-4}$, and that it is desired to reduce the fraction of A by a factor of 1000, to $x_W = 1 \times 10^{-7}$, while producing a "concentrated" product to $y_P = 0.01$, that is, concentration by a factor of 100.

It is desired to determine process requirements to achieve these separations for a specified feed rate.

SINGLE-STAGE LIMITATIONS

For a single ideal perfect-mix stage with specified α^*, the actual stage separation (i.e., α_i) will depend on stage cut θ as well as on r. The single perfect-mix stage extent of separation for α^* = 2.75, 10, 100, and 1000 as a function of stage cut for various r for the two feed compositions was calculated by solving the appropriate "equilibrium" and material balance equations. Table 1 shows y_i, x_i, the recovery $[R_i^A = (y_i)(H_i)/(z_i)(Z_i)]$, and α_i for a few combinations of α^*, r and θ, while Figs. 3 and 4, graphically

TABLE 1

Comparison of Separations That Can Be Obtained in a Single Perfect-Mix Stage for Different α^*, (a) $r = 1000$, (b) $r = 20$, for Stage Cuts = 0.1 and 0.5 When $z_i = 0.5$, and 0.0001.

(a)

SINGLE PERFECT-MIX STAGE SEPARATION, r = 1000

	zi =	0.5				zi =	0.5		
	θ =	0.1				θ =	0.5		
α*	yi	xi	Ri^A	αi	α*	yi	xi	Ri^A	αi
2.75	0.7141	0.4762	0.1482	2.747	2.75	0.6237	0.3763	0.6237	2.747
10	0.8933	0.4563	0.1787	9.98	10	0.7595	0.2405	0.7595	9.97
100	0.9877	0.4458	0.1975	99.8	100	0.9087	0.9013	0.9087	99.0
1000	0.9987	0.4446	0.1998	997.8	1000	0.9689	0.0311	0.9689	968.9
	zi =	0.0001				zi =	0.0001		
	θ =	0.1				θ =	0.5		
2.75	0.0002337	8.51E-05	0.2337	2.745	2.75	0.0001466	5.34E-05	0.7330	2.745
10	0.000524	5.29E-05	0.524	9.91	10	0.0001817	1.83E-05	0.9083	9.91
100	0.0009099	1E-05	0.9099	91.0	100	0.0001978	2.17E-06	0.9891	90.99
1000	0.000982	1.96E-06	0.9823	500.5	1000	0.000198	3.96E-07	0.9898	500.3

(b)

SINGLE PERFECT-MIX STAGE SEPARATION, r = 20

	zi =	0.5				zi =	0.5		
	θ =	0.1				θ =	0.5		
α*	yi	xi	Ri^A	αi	α*	yi	xi	Ri^A	αi
2.75	0.7502	0.4772	0.1410	2.62	2.75	0.6176	0.3824	0.6176	2.61
10	0.8849	0.4572	0.1770	9.13	10	0.7467	0.2535	0.7465	8.67
100	0.9862	0.4460	0.1972	89.05	100	0.8867	0.1133	0.8867	62.26
1000	0.9987	0.4458	0.1998	997.76	1000	0.9689	0.0311	0.9689	968.90
	zi =	0.0001				zi =	0.0001		
	θ =	0.1				θ =	0.5		
2.75	0.000219	8.67E-5	0.2193	2.53	2.75	0.000143	5.67E-5	0.7166	2.53
10	0.000434	6.29E-5	0.4338	6.90	10	0.000175	2.53E-5	0.8734	6.90
100	0.000651	3.87E-5	0.6512	16.82	100	0.000189	1.12E-5	0.9438	16.81
1000	0.000916	4.67E-5	0.9162	19.64	1000	0.000198	1.01E-5	0.9898	19.63

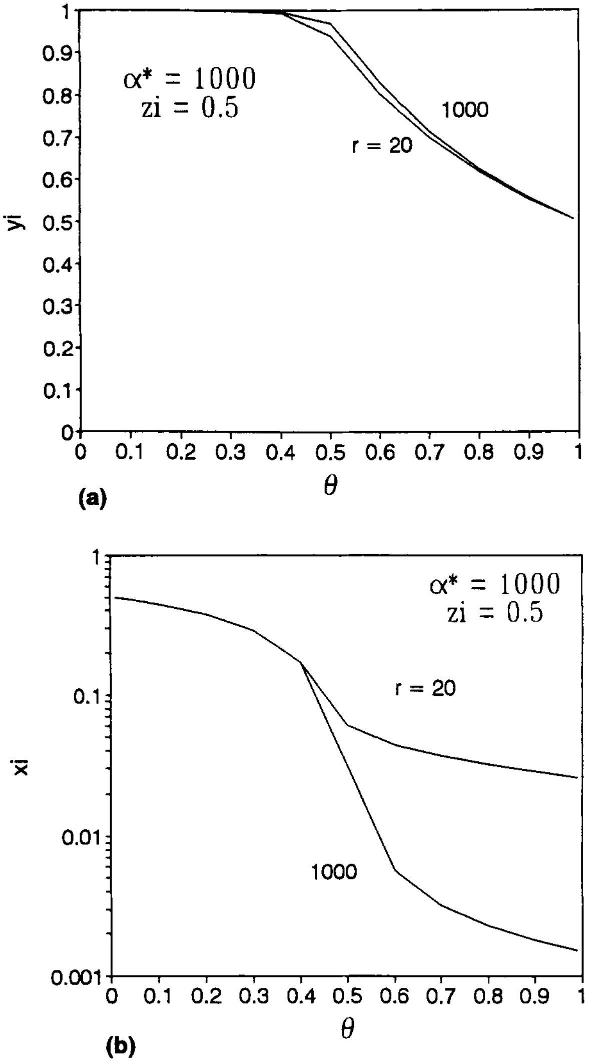

FIG. 3 Separation parameters as a function of stage cut in a single perfect-mix stage for $r = 20$ and 1000, $\alpha^* = 1000$, $z_i = 0.5$.

present this information for the case of $\alpha^* = 1000$ for the two desired separations.

As can be seen from the results of the single-stage calculations, the greatest enrichment in the heads stream occurs at small values of θ, but

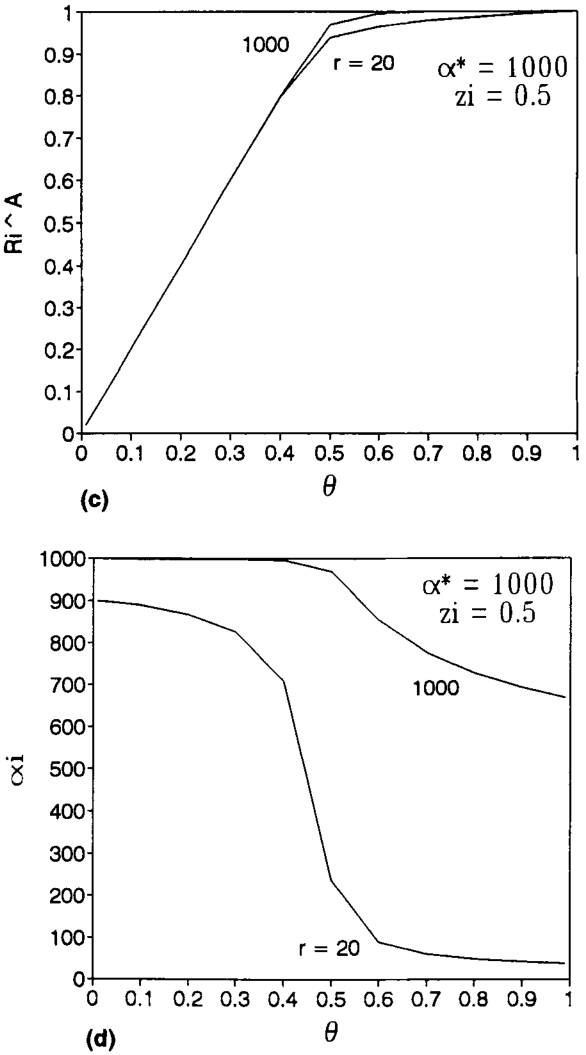

FIG. 3 Continued.

most of the A remains in the tails stream at small θ, that is, the recovery is small. Significant single-stage enrichment and recovery only occurs at very large α*, but, as can be seen, there can be significant limitations on the separation that can be obtained in the single stage even with large α*.

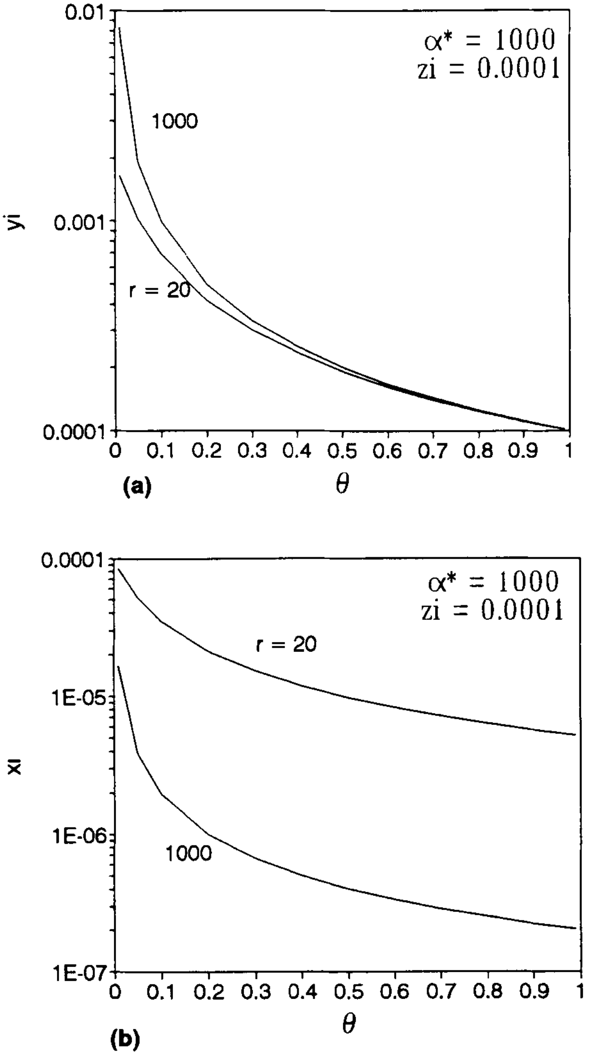

FIG. 4 Separation parameters as a function of stage cut in a single perfect-mix stage for $r = 20$ and 1000, $\alpha^* = 1000$, $z_i = 0.0001$.

For example, neither of the desired separations of $y_P \geq 0.99$, and $x_W \leq 0.01$ for $z_i = 0.5$, nor $x_W \leq 1 \times 10^{-7}$, $y_P \geq 0.01$, when $z_i = 1 \times 10^{-4}$ can be met in the single stage even with $\alpha^* = 1000$, $r = 1000$! This indicates that, in most cases, cascading will probably be required to meet desired separations regardless of the magnitude of α^*.

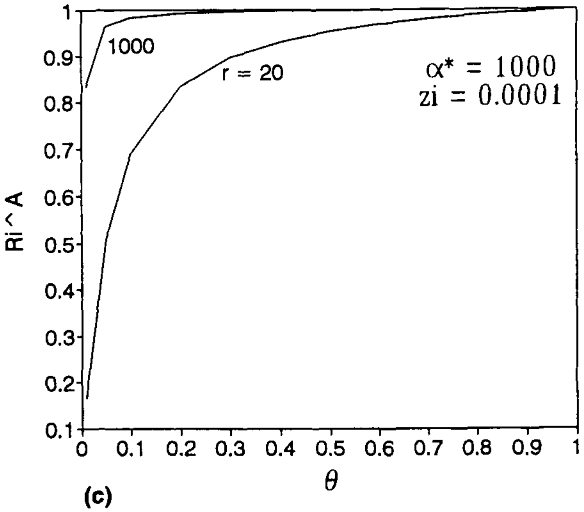

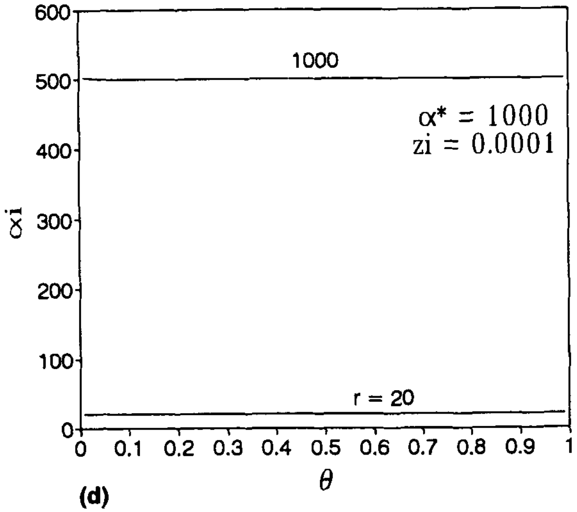

FIG. 4 Continued.

COUNTERCURRENT RECYCLE MEMBRANE CASCADES

Since the single-stage separations are limited, cascading is required to produce a "large" separation, especially with smaller values of α^*. Only countercurrent recycle cascades (CRCs) will be considered in this study.

The distinguishing feature of a CRC is the recycle flow pattern within the cascade: the feed to each stage (except for the two end, or "product" stages) consists of the heads from the next lower stage and the tails stream from the next higher stage. This recycle flow pattern is approached in a continuous distillation column and is used in gas diffusion cascades and separation cascades based on isotope exchange reactions between gas and liquid phases, etc.

A schematic diagram for the conceptual design of a 5-stage CRC to separate a binary mixture of ion pairs based on permeation through ILMs is shown in Fig. 5. Depending on α*, and specific cascade design, more (or less) than 5 stages may be required to effect the separations of interest in this study.

In this design the cascade feed, rate F with ion concentration C_F^t and ion fraction x_F is introduced at an intermediate point within the cascade, preferably at a point where the feed to the stage (i.e., the tails stream from the next higher numbered stage) is the same composition as the cascade feed composition. The cascade process results in an overall separation which produces a product, rate P, enriched in the desired species to y_P, and a "waste" product stream rate W, reduced in the desired species to composition x_W. For a binary ion solution with all $\alpha_i > 1$, any value of y_P and x_W (consistent with feed composition) may be obtained in the single cascade provided the CRC is designed properly, that is, with sufficient interstage (recycle) flows and number of stages. The required number of stages and interstage flow rates depend on the α_i, x_F, and the desired

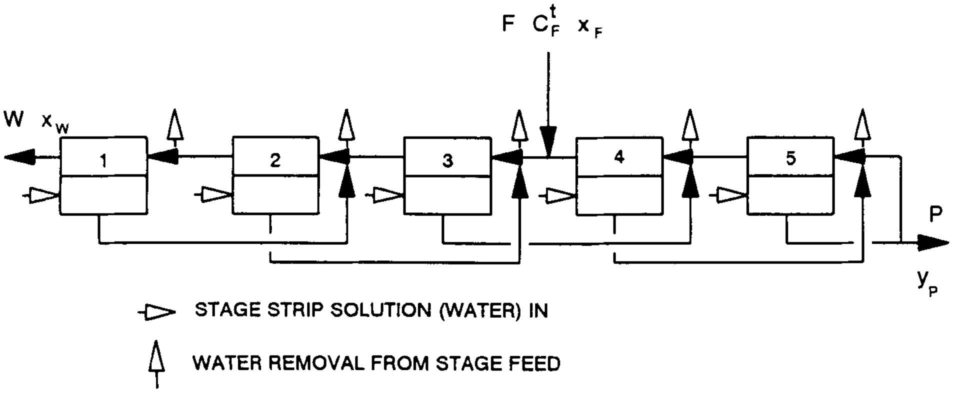

FIG. 5 Schematic diagram of a countercurrent recycle cascade for ion permeation.

x_W and y_P. Multicascade systems will be required for multi-ion systems to produce the different highly enriched species.

As previously discussed, a relatively high concentration of ions must be maintained on the "feed" side, while a relatively low concentration must be maintained on the "strip" side of the membrane stages. In this preliminary conceptual design this stagewise concentration difference is accomplished by using deionized water as inlet strip solutions to each stage, i.e., $(C^t{}_S)_{i,\text{in}} = 0$. Since the feed to a stage consists of the tails stream from the next higher numbered stage, combined with the heads stream from the next lower numbered stage, for a general stage i the outlet strip phase (the heads stream) from stage $i - 1$ must be concentrated to reestablish the required feed concentration. In addition, since total ion concentration is reduced on the feed side of each stage by the permeation process, water must also be removed from the tails stream from stage $i + 1$ to reestablish the required high stage feed concentration. This solvent removal from stage heads and tails streams is indicated by the vertical open arrows in the diagram. In practice it might be advantageous to combine the appropriate heads and tails streams before solvent removal, that is, solvent is removed from the combined feed to each stage.

This concentration process within the cascade could probably be carried out in at least three ways: evaporation, or freezing, which would make the overall process thermally driven, or reverse osmosis, which would make it mechanical energy driven.

Cascade theory specific for ion permeation is only now being developed since multi-stage (countercurrent recycle cascade) theory apparently has not been applied to ion permeation previously. However, just as with the single-stage calculations, concepts similar to CRC theory in gas diffusion and permeation must apply, including the concepts of minimum number of stages, minimum recycle ratios, and the *ideal* cascade.

Note that a general CRC is depicted in Fig. 5, where a quantity of enriched product, composition y_P, is returned as recycle to stage N.

For other separation processes with constant α_i that are carried out in CRCs (i.e., distillation, gas diffusion, isotope exchange reaction, etc.), the *ideal* cascade design results in the minimum total interstage flow requirements to effect a specified separation. Although, in general, the number of stages required to make the separation will be greater for an ideal cascade than for other (constant recycle) designs, the minimization of TISF minimizes the overall cascade *size* required to make the separation. At this time it is not known whether or not ideal cascade theory can be rigorously applied to ion permeation since there will, in general, be stagewise variation in the stage separation factors. However, *no-mix* cascades can certainly be designed, and for this "first look" at cascade requirements for ion permeation it is convenient to consider no-mix CRCs which may approach the performance of ideal cascades. In this case the term "no-mix" refers to cascades designed so that the heads and tails streams that make up the feed to each stage have the same compositions; that is, $y_{i-1} = x_{i+1}$, while at the feed stage $x_F = y_{F-1} = x_{F+1}$. Only no-mix CRCs composed of perfect mix stages will be considered in this study.

Note that for the no-mix cascade, recycle is not returned to stage N, and P is the entire permeate from stage N, as shown in Fig. 6. Otherwise the cascade no-mix criteria cannot be met.

Many no-mix designs are possible, depending on the value of the heads separation factor assumed at the feed stage (9). For cascades with constant α_i, an ideal cascade results when all $\beta_i = \sqrt{\alpha_i}$, hence for the present calculations a reasonable design assumption for the no-mix ion permeation cascade is that $\beta_F = \sqrt{\alpha_F}$. Thus, for this "first look, the following conditions are assumed, which, together with Eq. (10) or (11), fix all cascade stream compositions:

$$x_F = y_{F-1} = x_{F+1}$$

$$\beta_F = \frac{y_F(1 - z_F)}{z_F(1 - y_F)} = \sqrt{\alpha_F}$$

$$y_{i-1} = x_{i+1}$$

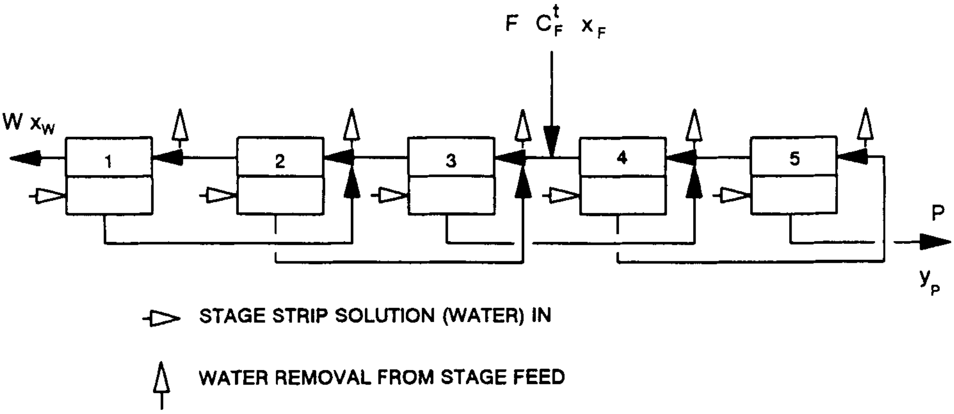

FIG. 6 Schematic diagram of a no-mix countercurrent recycle cascade for ion permeation.

NO-MIX CASCADE CALCULATIONS AND RESULTS

Using the above assumptions, calculations for no-mix cascades are conveniently made by computer using a spreadsheet program. The calculations are made starting at the feed stage, and calculating stream compositions "up" in the enriching section to a stage where $y_i \geq y_P$, and "down" in the stripping section to a stage where $x_i \leq x_w$, using the appropriate "equilibrium" and material balance equations. However, α_F depends on y_F, which is fixed by the assumed β_F. In addition, only a discrete number of ideal stages in the cascade are considered, and so, in general, y_P and x_W cannot be exactly specified. Thus, an iterative procedure is required to both find the number of stages to make the specified separation and to determine the β_F to give $\beta_F = \sqrt{\alpha_F}$. Note that the β_F must be in the range $1 < \beta_F < \alpha_F$ in order for separation to occur on the stage.

Using the calculated stage compositions for a specified feed rate, overall material balances fix W and P, while material balances around stripping and enriching sections of the cascade fix all internal cascade stage rates.

The results of calculations for $\alpha^* = 2.75$, 10, 100, and 1000, and for $r = 20$ and 500 for the two specified separations are presented in Tables 2 and 3. Assumptions, units, and nomenclature for the calculated data presented in these tables are:

- $(C^t_F)_i = 10$, $(C^t_S)_i = 0.5$, 0.02 molar for $r = 20$ and 500
- $P^A = 0.95$ cm/h
- AREA = total cascade membrane area, m^2
- TSRR = total cascade solvent removal rate, L/h
- The following quantities are all on a solvent-free basis:
  - $F = 10$ g·mol/h
  - TISF = total interstage flow rate in the cascade, including P and W, g·mol/h
  - P, W, = product and waste stream rates, g·mol/h
  - x, y = mole fractions

It is thought that $r = 500$ may be about the highest "practical" concentration ratio considering the limited solubility of some salts. As can be seen from the calculated data presented in the tables, there are some deviations in the P, W, y_P, and x_W values for the various designs because the cascades were limited to a discrete number of stages. Notwithstanding these small deviations, practically the same separation is obtained in each specific design, and the comparisons made between designs are valid.

The number of stages required to make the specified separations vary from 24 ($\alpha^* = 2.75$, $x_F = 1 \times 10^{-4}$, $r = 20$ and 500) to 3 ($\alpha^* = 1000$,

TABLE 2

No-Mix Cascades, with $\beta_F = \sqrt{\alpha_F}$, Designed to Produce $y_F \geq 0.01$, $x_W \leq 1 \times 10^{-7}$ from $F = 10$, $z_F = 0.0001$, with $r = 20{,}500$

α^*	$(\alpha_i)_{av}$	N	P	Y_P	W	x_W	TISF	TSRR	AREA
				$r = 20$					
2.75	2.53	24	0.0975	0.0102	9.902	9.5E−8	1,335.4	516.5	7.9
10	6.90	12	0.0807	0.0124	9.919	4.2E−8	392.1	96.5	6.5
100	16.87	8	0.0355	0.0281	9.964	8.6E−8	191.2	46.4	23.5
1,000	19.74	8	0.0260	0.0385	9.974	5.9E−8	166.0	42.1	185.4
				$r = 500$					
2.75	2.63	24	0.0652	0.0152	9.935	8.6E−8	1,160.5	11,051	6.4
10	9.82	11	0.0340	0.0294	9.966	3.4E−8	309.7	1,769.5	4.5
100	83.66	6	0.0140	0.0717	9.986	1.4E−8	139.4	753.7	15.7
1,000	335.5	4	0.0303	0.0330	9.970	1.6E−8	594.0	594.0	123.7

TABLE 3

No-Mix Cascades, with $\beta_F = \sqrt{\alpha_F}$, Designed to Produce $y_F \geq 0.01$, $x_W \leq 0.01$ from $F = 10$, $z_F = 0.5$, with $r = 20,500$

α^*	$(\alpha_i)_{av}$	N	P	Y_P	W	x_W	TISF	TSRR	AREA
				$r = 20$					
2.75	2.60	19	4.992	0.9924	5.0077	0.0091	861.2	438.1	4.1
10	8.42	9	4.986	0.9962	5.0140	0.0065	229.5	120.7	2.5
100	58.48	5	4.972	0.9986	5.0279	0.0069	120.2	59.5	9.2
1,000	298.32	4	4.990	0.9989	5.0101	0.0031	108.4	48.7	96.8
				$r = 500$					
2.75	2.74	19	5.000	0.9936	5.000	0.0064	822.9	10,246	3.7
10	9.92	9	5.000	0.9968	5.000	0.0033	218.5	2,656.1	2.2
100	94.61	5	5.000	0.9999	5.000	0.0012	113.5	1,177.7	7.3
1,000	811.51	3	4.995	0.9990	5.005	0.0020	71.9	791.4	56.4

$x_F = 0.5, r = 20$). In accordance with the previous discussions concerning the effects of r and x_i on α_i for specified α^*, the average stage separation factor, $\Sigma\alpha_i/N$, in the various cascade designs deviates considerably from α^*. The deviation is greater with larger α^* and smaller r, and for the separation of the more dilute feed solution. This deviation is particularly evident for $\alpha^* = 100$ and 1000, $r = 20$ for the $x_F = 1 \times 10^{-4}$ separation, where the $(\alpha_i)_{ave} = 16.87$ for $\alpha^* = 100$, and $(\alpha_i)_{ave} = 16.87$ for $\alpha^* = 100$, and $(\alpha_i)_{ave} = 19.74$ for $\alpha^* = 1000$. As a result, these two cascade designs require the same number of stages (8) to make the specified separation.

Both required TSRR and TISF to decrease with increasing α^* [and $(\alpha_i)_{ave}$]. However, the total cascade membrane area (Σa_i) required to make the separations is a minimum at $\alpha^* = 10$ for the cases considered. The stagewise areas were calculated from Eq. (1), and the required areas reflect the stagewise driving force for diffusion, $[x_i(C_F^t)_i - y_i(C_S^t)_i]$, relative to the strip side concentration, $y_i(C_S^t)_i$, and the magnitude of P^A. For these calculations the P^A is the value that was determined experimentally for $CsNO_3$ diffusion through an octanol membrane (7). It should be noted that macrocycle transport usually results in P^A values considerably less than for ordinary diffusion since the membrane phase is chosen to try to eliminate ordinary diffusion, and the rate of diffusion of the very large carrier molecules complexed with the target ions is slower than for ordinary diffusion.

Although not shown in the present illustration, for fixed r the area increases as $(C_S^t)_i$ decreases. This is because, for the same r, the actual driving force for diffusion is less for the lower $(C_S^t)_i$. In addition, for all $(C_S^t)_i$, the area increases as r is decreased since this also results in a decreased driving force. At low enough r the driving force becomes zero, and $a_i \rightarrow \infty$. For the two r investigated in this study, the required total membrane area increased with decreasing r.

The TSRR is a measure of the amount of energy input required to "drive" the separation cascade. It decreases with increasing α^*, but is greater for increasing r.

The complex response to the design variables of r, $(C_F^t)_i$, and $(C_S^t)_i$ indicate that optimization would be possible for ion permeation applied to specific separations. This was beyond the scope of the present study.

GENERAL DISCUSSION

The derivation of the equations presented in this paper is based on the assumption that Fick's law adequately describes the permeation of dissociated salts from solution through ILMs by both passive (ordinary) diffusion and macrocycle-mediated cation transport. Since transport models based on Fick's law have been used to analyze the results of laboratory transport experiments in ILMs, Eqs. (1)–(12) should be valid, at least for a preliminary study of the engineering design and analysis of single perfect-mix stages, and to determine membrane cascade requirements to achieve specific separations. These equations are very similar to equations that have been developed to model gas permeation stages and cascades, with the concentration ratio being analogous to the pressure ratio in gas permeation. The calculations based on Fick's law clearly show that severe limitations on stage separations can result from unfavorable feed/strip concentration ratios, and/or by the requirement to strip the feed stream to very low mole fractions, even for systems that exhibit very high α^*. However, the designs presented in this paper must still be considered to be conceptual in nature; their validity has not been tested in practice.

Many other perfect-mix stage cascade designs are possible that would accomplish the desired separations (i.e., constant recycle rather than no-mix), but it is thought that the no-mix design with $\beta_F = \sqrt{\alpha_F}$ represents cascade designs that approach minimum TISF requirements to make the specified separations.

Other stage designs with different flow patterns (for example, countercurrent or cocurrent flow with no mixing, and crossflow stages) are possible, and these flow configurations may be more efficient than the perfect-mix stages. An investigation of these other stage flow patterns may be the topic of a future investigation. However, with respect to perfect-mix stages, the following significant conclusions can be made based on the present study.

1. Separation cascades based on ion permeation necessarily must be quite complex because both heads and tails streams that make up the feed in the stages in the cascade must be reconcentrated by solvent removal. As a result, the overall cascade process may be very energy intensive.
2. Ion permeation cascades based on ordinary or passive diffusion will require many stages to effect many desired separation because of low α^*.
3. Cascading will be required to effect many separations even for systems with large α^* such as may be obtained using macrocycle-mediated transport.
4. There can be severe diffusional limitations that result in low α_i if r is small, or when the separation must produce very small x_i regardless of the magnitude of α^*.

ACKNOWLEDGMENT

This project was partially funded by the INEL University Research Consortium. The INEL is managed by Lockheed Martin Idaho Technologies Company for the US Department of Energy, Idaho Operations Office, under Contract DE-AC07-94ID13223.

REFERENCES

1. R. Bloch, in *Membrane Science and Technology* (J. E. Flin, Ed.), Plenum, New York, NY, 1970, pp. 171–187.
2. S. A. Stern and W. P. Walawender, "Analysis of Membrane Separation Parameters," *Sep. Sci., 4*(2), 129–159 (1969).
3. M. Benedict, T. H. Pigford, and W. H. Levi, *Nuclear Chemical Engineering*, 2nd ed., McGraw-Hill, New York, NY, 1981, Chap. 12.
4. M. Benedict, "Multistage Separation Processes," *Trans. Am. Inst. Chem. Eng., 43*(2), 41–60 (1947).
5. R. W. Naylor and P. D. Backer, "Enrichment Calculations in Gaseous Diffusion: Large Separation," *AIChE J., 1*(1), 95–99 (1955).
6. J. F. Dozol, J. Casas, and A. M. Sastre, "Influence of Extractant on Strontium Transport from Reprocessing Concentrate Solutions through Flat-Sheet Supported Liquid Membranes," *Sep. Sci. Technol., 29*(15), 1999–2018 (1994).
7. J. D. Parks, "Separation of Cesium and Strontium from Nuclear Waste by Supported Liquid Membranes," M. S. Thesis in Chemical Engineering, Montana State University, Bozeman, MT, 1995.
8. R. M. Izatt, M. P. Biehl, J. D. Lamb, and J. J. Christensen, "Rapid Separation of Tl^+ and Pb^{2+} from Various Binary Cation Mixtures Using Dicyclohexano-18-crown-6 Incorporated into Emulsion Membranes," *Sep. Sci. Technol., 17*(11), 1351–1360 (1982).
9. R. S. Herbst and F. P. McCandless, "No-Mix and Ideal Separation Cascades," *Ibid., 29*(17), 2215–2226 (1994).

Received by editor November 5, 1996
First revision received January 1997
Second revision received March 1997